AlGaN/GaN two-dimensional electron gas heterostructures on 200 mm diameter (111)-oriented silicon substrates

S. Tripathy,[1, a)] Vivian K. X. Lin,[1] S. B. Dolmanan,[1] M. K. Kumar,[1] Joyce P. Y. Tan,[1] Shane Todd,[2] Veeco,[3] Veeco,[3] D. L. Kwong,[2] G. Q. Lo[2, b)]

[1]*Institute of Materials Research and Engineering, A*STAR (Agency for Science, Technology and Research), 3 Research Link, Singapore 117602*

[2]*Institute of Microelectronics, A*STAR (Agency for Science, Technology and Research), 1 Science Park Drive, Singapore*

[3]*Veeco Instruments Inc., 394 Elizabeth Ave., Somerset NJ 08873, USA*

The authors report on the epitaxial growth and characterization of crack-free AlGaN/GaN heterostructures on 200 mm (111)-oriented silicon substrates. The total nitride stack thickness grown by the metal-organic chemical vapor deposition (MOCVD) technique is about 3.6 ± 0.1 μm. The structural and optical properties of these layers are studied by cross-sectional scanning transmission electron microscopy, high-resolution x-ray diffraction, photoluminescence, and micro-Raman spectroscopy measurements. An average threading dislocation density of the order of 1.25×10^{9} cm^{-2} is estimated on the surface of these nitride structures grown on such a large area silicon platform. A comparatively large wafer bowing correlates well with the in-plane stress measured from the Raman measurements. The top AlGaN/GaN interfaces reveal the formation of a two-dimensional electron gas (2DEG) with an average sheet resistivity of 350 Ω/sq, a sheet carrier concentration of 1.02×10^{13} cm^{-2}, and an average mobility value of 1500 cm^2/Vs. The experimental results show immense potential of 200 mm GaN-on-silicon technology for electronic devices.

[a)]Email: tripathy-sudhiranjan@imre.a-star.edu.sg

[b)]Email: logq@ime.a-star.edu.sg

Recently, Gallium nitride (GaN) based solid-state devices have shown exceptional capabilities for electronic devices operating at high power, high-frequency, and high-temperature. The fundamental properties of AlGaN/GaN material system also make it an ideal candidate for high-power microwave devices. However, a large scale deployment of GaN electronic devices in consumer market applications requires a reduced cost. Due to the lack of commercially available large area GaN substrates, GaN heterostructures are currently grown primarily on sapphire, silicon (Si), and silicon carbide (SiC). For electronic applications, Si substrate is a very attractive alternative, being much cheaper than sapphire and SiC when substrate diameters are higher than 150 mm. There has been lot of interest to grow III-nitride heterostrutures on silicon substrates due to the tremendous market potential to be integrated with well-developed Si microelectronic circuit technologies.[1-3] However, the GaN on Si epitaxy suffers from a significant mechanical strain that is caused by the lattice mismatch, a large difference in thermal expansion coefficients between substrate and epilayers, and the thermal gradients through the wafers. These result in high density of misfit and threading dislocations (TDs) in the AlGaN/GaN heterostrutures grown on Si substrates. Beside the tensile stress generated in GaN epitaxial wafers on Si, the large diameter wafers show a pronounced bowing effect leading to non-uniform electronic properties. To relieve the tensile stress and to achieve crack-free GaN heterostrutures, a wide variety of buffer and inter layers such as low-temperature AlN,[4] graded AlGaN buffers,[5] and Al(Ga)N/GaN superlattices[6] have been used. For integration with Si Foundries based on complimentary metal-oxide-semiconductor (CMOS) technologies, it is desirable to scale up GaN epitaxy to 200 mm Si substrates. However, ~~till~~ to date there ha~~sve~~ been less success in achieving high quality AlGaN/GaN heterostruture ~~over~~ on 200 mm Si substrates due to issues like epi~~a~~layer cracking, wafer bowing, and high density of point and line

defects when nitride stack thickness exceeds 3.0 µm. To showcase high electron mobility transistors (HEMTs) on 200 mm Si platform with comparatively similar device performances levels as reported currently on Si substrate platform,[7, 8] it is necessary to grow thicker GaN buffer to minimize the buffer leakage and also to improve the layer crystalline quality. In this letter, we ~~show~~ report crack-free AlGaN/GaN heterostructures ~~on~~ grown on 1mm thick, 200 mm diameter (111)-oriented silicon substrates and present an in-depth characterization study of epilayers grown by MOCVD. ~~with a~~ The ~~-~~GaN buffer is ~2.5 µm thick (total nitride stack thickness >3.5 µm) ~~using a Veeco K465i TurboDisc MOCVD tool. and present an in-depth characterization study of epilayers grown by MOCVD~~. The optical, electronic, and structural properties of the layers show their suitability for electronic devices.

The epitaxial growth of GaN on 1.0 mm thick Si (111) substrates was carried out in a Veeco Turbodisc K465i high throughput MOCVD tool equipped with a DRT 210 in-situ process monitor. The starting Si(111) substrate with resistivity (..xxxx.. ohm cm) was heated to ~1000 °C in H_2 atmosphere and annealed for about 3 min to remove native oxide from the surface. First, a high temperature AlN buffer (thickness 100-110 nm) was grown followed by five AlGaN buffer layers with an Al content grading from 20 to 80%. Next, the GaN layer with a thickness ~2.5 µm on top of the graded buffers was overgrown with two thin strain-compensating AlN interlayers.[4] In order to make GaN semi-insulating for electronic applications, carbon doping has been used. About 18 to 20 nm thick target AlGaN barrier layer with a 2 nm thin GaN cap was grown to form a 2DEG interface. The layer thicknesses of the epilayers, the buffer and interlayers, as well as the top $Al_xGa_{1-x}N$ layers were determined using a Philips FEI CSM 300 transmission electron microscopy (TEM) set up. To analyze the crystalline quality of the as-grown layer structure, high resolution x-ray diffraction (HRXRD) measurements were performed with a PANalytical X'Pert

PRO diffractometer using a 4-bounce hybrid mirror monochromatized Cu Kα1 radiation (λ = 1.5406 Å) and an open detector for the ω and ω–2θ scans. HRXRD measurements were performed to obtain the full-width at half-maximum (FWHM) of x-ray rocking curves of various symmetrical and asymmetrical Bragg reflections and a quantitative evaluation of dislocation densities was also performed. The dislocation density was further confirmed by the etch pit densities of the samples evaluated by performing hot phosphoric acid etching followed by atomic force microscopy (AFM). Variable temperature micro-photoluminescence (PL) measurements were performed to probe the optical quality of the 2DEG at the top surface. The characteristics of optical phonons originating from such 2DEG AlGaN/GaN interfaces were probed by variable temperature UV micro-Raman measurements using a Jobin Yvon LABRAM-HR setup. The electrical properties of the 2DEG structures were probed by Hall effect measurement system.

Figure 1 shows the cross sectional TEM micrographs of the AlGaN/GaN heterostructure grown on 200 mm Si substrate. Two sets of measurements were performed to check the total nitride stack thickness including the AlN starting buffer, graded multiple AlGaN buffer layers, the low-temperature (LT) AlN interlayers, and top AlGaN/GaN interfaces. To probe AlGaN/GaN 2DEG interfaces and the nature of dislocation propagation, we have also explored imaging of high-angle annular dark-field scanning transmission electron microscopy (HAADF-STEM). The z-contrast HAADF-STEM images show the crystalline nature of the Al(Ga)N epilayers and accurate thickness profiles. An average thickness of about ~3.6 µm nitride stack is confirmed from TEM data. High resolution TEM imaging shown in Fig. 1 also reveals ~18 ± 2 nm $Al_xGa_{1-x}N$ barrier layer with a thin ~2.0 nm GaN cap. The thickness of two LT-AlN interlayers within the thick GaN template is about 10 - 11 nm. The bright field HR-TEM shows clearly the five AlGaN buffer layers of total thickness ~1.0 µm. Deposition of AlN nucleation

layer on Si(111) before GaN growth has often used to avoid the diffusion of Ga into the substrate. Furthermore, the thermal expansion coefficients of AlN is between those of GaN and Si and hence to control strain balance on the large area wafer, we have used five graded $Al_{1-x}Ga_xN$ buffer layers (x = 20 to 80%). The LT-AlN interlayers are grown at an intermediate temperature of 860 °C. The LT-AlN interlayer offers in-plane compressive stress because of the ~2.5% lattice mismatch between the AlN and GaN, and usage of such multiple interlayers helps to partially offset the thermal tensile stress during temperature ramp-down.[9] Thus, the use of bottom AlGaN/AlN buffers and LT-AlN eventually led to realization of a crack-free 200 mm AlGaN/GaN heterostruture on a 1 mm thick Si(111) substrate.

With this substrate thickness and post growth in-plane stress gradient introduced, we have measured a wafer bowing of about 125 µm and curvature of 24 km^{-1}. ~~This bowing~~These values are~~is~~ relatively higher when we compare to ~~a~~ bowing and curvature values of about 40 µm and 15 km^{-1} ~~–~~respecitively measured from a similar 150 mm AlGaN/GaN heterostructure (total nitride thickness 2.9 µm) on 1.0 mm thick Si(111). However, this is quite comparable to reported results on a thinner 200 mm GaN template.[7] In addition, the compressive strain field in the interlayer also leads to dislocation bending and annihilation of some screw dislocations as seen from TEM imaging. ~~However, s~~At the same time, some lattice mismatch induced misfit dislocations also appear at these interfaces, propagating to the top AlGaN barrier layer. In order to estimate the average threading dislocation (TD) density in such 200 mm epiwafers, we have further explored the HRXRD and AFM measurements. In addition, we have seen a wafer bowing in excess of 100 µm which could result in non-uniform electronic properties of the 2DEG interfaces due to an expected variation of Al content and in-plane stress. Therefore, micro-

Formatted: Superscript

Raman, micro-PL, and Hall measurements were performed across the epiwafer to estimate such variation associated with wafer bowing.

Figure 2a shows a post-growth picture of the 200 mm wafer with AlGaN/GaN epitaxial structure on the surface. Figure 2b shows a typical HRXRD ω-2θ scan of (0002) diffraction plane of epitaxial AlGaN/GaN structures on 200 mm Si. The spectrum shows clear satellite peaks at lower Bragg angle side representing good crystalline quality interfaces. The dominant peak is from the thick GaN layer, while the peaks at higher Bragg angles originate from the $Al_xGa_{1-x}N$ and AlN layers. The inset shows the rocking curves of (002) and (102) diffraction planes of such thick GaN layer. The full width at half maximum (FWHM) measurements of the XRD rocking curves of (002), (102) and (105) are~~is~~ about 527, 1248, and 813 arcsecs, respectively, which are~~is~~ comparable to GaN crystal quality reported in literature for such 2DEG heterostrutures on a 150 mm Si substrate.[8] The FWHM of x-ray rocking curves of the symmetrical and asymmetrical Bragg reflections are also studied, and a quantitative evaluation of threading dislocation (TD) densities is carried out using the Hordon and Averbach model.[10] By plotting the square of the FWHM of each rocking curve of reflections against tan2θ, where θ is the Bragg angle, a linear plot is fitted to estimate an average TD density (D) from the y-intercept of the plot, using the relation $D = y - \text{intercept}/4.36b^{2,}$ where b is the length of the Burgers vector (b_{screw} = 0.5185 nm, b_{edge} = 0.3189 nm).

The screw and edge dislocation densities are then calculated from the plots using the data obtained from symmetrical and asymmetrical reflections, respectively. From our study, we estimated an average screw and edge dislocation density to be about 0.53×10^9 cm^{-2} and 1.5×10^9 cm^{-2}, respectively. It is well known that mainly three types of TDs: pure-edge, pure screw, and mixed-type, dominate~~s~~ the MOCVD grown GaN epialyer and the HRXRD technique usually

collects information from the whole GaN stack. To further complement the dislocation density at the top 2DEG interfaces, we have carried out estimation of etch pit density. In AFM micrographs of GaN surfaces, the pure-edge TDs are typically merged into the terraces while step terminations are usually associated with screw/mixed TDs. The AFM imaging gives a root mean square roughness of about 0.2 – 0.3 nm on the as-grown surface. The etch pit density at the top surface is studied after hot phosphoric acid etching and AFM imaging. From the AFM images of the as-grown and etched samples, the etch pits are mostly found at the step terminations. Hence, we consider the etch pit densities to be mostly screw/mixed type TDs, and are estimated to be about 1.25×10^{9} cm^{-2} agreeing closely with the TD density calculations from the HRXRD measurements.

In order to address the optical properties of the 2DEG hetero-interfaces, we have carried out micro-PL and micro-Raman measurements. The emission from top AlGaN barrier is studied using ultraviolet (UV) PL spectra excited using 266 nm laser. The multiple peak spectral deconvolutions give rise to peaks originating from the top AlGaN barrier and underlying GaN 2DEG channel. As expected, due to a relatively large wafer bowing, a linescan across the full 200 mm wafer shows that the much broader and weaker room-temperature PL peak from AlGaN varies from 340 nm (3.647 eV) to 350 nm (3.542 eV), whereas the stronger PL peak centered around 3.402 eV appears from the underlying GaN layer. PL peak from GaN using both 266 and 325 nm laser excitations show a variation from 3.402 to 3.410 eV across the wafer and such a variation is related to the presence of in-plane biaxial stress in the nitride stack. A relatively large variation of AlGaN peak is due to the combination of a fluctuation in Al content and the significant red shift due to a presence of a biaxial tensile stress. Figure 3 shows the variable temperature PL spectra recorded close to the wafer center. At 77 K, the strong PL peak at 3.454

eV corresponds to a near-band-edge free exciton transition from GaN while the broad peak located at 3.562 eV corresponds to the emission from top thin $Al_xGa_{1-x}N$ barrier layer. Due to the tensile stress induced at the top 2DEG interfaces, a significant red shifted PL peak is observed. The PL line scan across the 200 mm wafer using 325 nm excitation shows a ~~much~~ very uniform spectral intensity distribution of GaN band-edge and much weaker deep level yellow luminescence, thus representing good crystalline quality at the 2DEG GaN channel region.

To study the 2DEG interface properties, we have performed UV micro-Raman spectroscopy. The 325 nm UV Raman near-resonantly excites the top $Al_xGa_{1-x}N$/GaN interfaces. Figure 4a shows the Raman spectra recorded from the 200 mm AlGaN/GaN wafer under z(x,_)-z polarization geometry. The Raman spectra are excited with a low laser power to avoid thermal red shift. Beside the typical GaN E_2-high mode at 566 cm^{-1}, the Raman spectra are dominated by peaks at 600, 727, and 772 cm^{-1}. A variation of stress in the nitride layers due to a large wafer bowing factor leads to a significant change in the GaN E_2-high phonon peak position. The softening of the E_2-high optical phonon peak from the strain-free peak value (567.5 cm^{-1}) recorded from a freestanding GaN substrate, reveals the presence of a biaxial tensile stress. Using the relationship between in-plane stress and E_2-high peak shift, the UV Raman data across the 200 mm wafer show an average tensile stress of 0.46 GPa induced in the nitride layer.[11] Figure 4b presents the variable temperature Raman spectra from such an AlGaN/GaN heterostructure. The low-temperature spectra could clearly distinguish all Raman active modes. The weak feature around 700 cm^{-1} can be attributed to a disorder-activated mode related to lattice defects at the AlGaN/GaN interfaces.[12] The other two modes at 600 and 727 cm^{-1} are the interface modes from AlGaN/GaN system.[13] The interface mode at 727 cm^{-1} appears at the expense of the A_1(LO) phonon of GaN and represents the 2DEG nature of the hetero-interface.

The temperature-induced shifts of the two interface modes are opposite (from sample temperature variation of 77 K to 350 K) as such modes show an anti-symmetric potential and interact more strongly with free carriers. Furthermore, spectrum at 77 K clearly show the A_1(LO)-like phonon peak at 777 cm^{-1} originating from the thin AlGaN barrier. At low-temperature, the quasi-LO phonon from GaN also appears due to the top thin GaN cap interface inhomogeneity. The room- temperature deconvoluted A_1(LO) peak of AlGaN has been used to estimate the Al content using the relationship reported in Ref. 14 for samples with low Al content range when excited close to resonance. Using the experimental data and the relationship of AlGaN LO phonon peak vs Al content: $\omega_{LO}(x) = 734 + 356.8x - 814.7x^2$; average Al compositions of 15 ± 3% are obtained across the full wafer. Although Al composition fluctuation occurs due to a variation of biaxial stress in such a large wafer area, micro-Raman method addresses such local inhomogeneities across the full wafer. Such variation could be easily correlated to the wafer bowing and electrical characteristics across the 200 mm Si platform. To check the applicability of such AlGaN/GaN interfaces for high electron mobility transistors, Hall effect measurements are performed on the sample from center to edge. The sheet resistivity from the center to edge in such a 200 mm wafer shows an average value of 350 Ω/sq with a variation of about 15%, a maximum sheet carrier concentration of about 1.02×10^{13} cm^{-2}, and an electron mobility value of 1500 cm^2/Vs. Due to a strong wafer bowing and Al composition variation in the AlGaN barrier, the center to wafer edge mobility variation is about 20%. Such variations could be compensated with further improvement in our epitaxy and more exotic designs of interlayer spacing.

In summary, we report on the 200 mm AlGaN/GaN epiwafer development on Si substrate platform. An in-depth characterization study is presented to check the applicability of such

MOCVD grown material system for high-voltage electronics. The structural and optical characterization shows tremendous potential of such device grade GaN layers on silicon.

Acknowledgements: The authors thank funding support from TSRP SERC GaN-Si Power Electronics Program Project -102 169 0126.

References

[1]T. K. Li, M. Mastro, and A. Dadgar, *III–V Compound Semiconductors: Integration with Silicon-Based Microelectronics*, CRC Press, Parkway NW (2010).

[2]S. Arulkumaran, T. Egawa, and H. Ishikawa, Solid-State Electronics **49**, 1632 (2005).

[3]L. S. Selvaraj, A. Watanabe, and Takashi Egawa, Appl. Phys. Lett. **98**, 252105 (2011).

[4]A. Dadgar, J. Bläsing, A. Diez, A. Alam, M. Heuken, and A. Krost, Jap. J. Appl. Phys. Part 2 Lett. **39**, L1183 (2000).

[5]H. Marchand, L. Zhao, N. Zhang, B. Moran, R. Coffie, U. K. Mishra, J. S. Speck, S. P. DenBaars, and J. A. Freitas, J. Appl. Phys. **89**, 7846 (2001).

[6]E. Feltin, B. Beaumont, M. Laugt, P. de Mierry, P. Vennegues, H. Lahreche, M. Leroux, and P. Gibart, Appl. Phys. Lett. **79**, 3239 (2001).

[7]A. R. Boyd, S. Degroote, M. Leys, F. Schulte, O. Rockenfeller, M. Luenenbuerger, M. Germain, J. Kaeppeler, and M. Heuken, Physica Status Solidi C **6**, S1045 (2009).

[8]K. Cheng, M. Leys, S. Degroote, J. Derluyn, B. Sijmus, P. Favia, O. Richard, H. Bender, M. Germain, and G. Borghs, Jap. J. Appl. Phys. **47**, 1553 (2008).

[9]A. Dadgar, T. Hempel, J. Bläsing, O. Schulz, S. Fritze, J. Christen, and A. Krost, Physica Status Solidi C **8**, 1503 (2011).

[10]M. J. Hordon, and B. L. Averbach, Acta Metallurgica **9**, 237 (1961).

[11]S.Tripathy, Vivian K. X. Lin, S. Vicknesh, and S. J. Chua, J. Appl. Phys. **101**, 063525 (2007).

[12]V. Y. Davydov, I. N. Goncharuk, A. N. Smirnov, A. E. Nikolaev, W. V. Lundin, A. S. Usikov, A. A. Klochikhin, J. Aderhold, J. Graul, O. Semichinova, and H. Harima, Phys. Rev. B **65** 125203 (2002).

[13]V. K. X. Lin, S. B. Dolmanan, S. L. Teo, H. H. Kim, E. Alarcon-Llado, A. Dadgar, A. Krost, and S. Tripathy, J. Phys. D: Appl. Phys. **44**, 365102 (2011).

[14]M. Yoshikawa, J. Wagner, H. Obloh, M. Kunzer, and M. Maier, J. Appl. Phys. **87**, 2853 (2000).

Figure Captions:

FIG. 1. Cross-sectional TEM images of the AlGaN/GaN heterostructures and full nitride stack on a AlN nucleation layer on Si(111). (a) and (b) represent bright-field XTEM of layers and the top AlGaN/GaN interfaces. (d) and (e) represent the HAADF-STEM z-contrast images of the same sample showing different interfaces and much accurate thickness profiles.

FIG. 2. (a) Picture of the 200 mm GaN-on-Si wafer after growth. (b) HRXRD ω-2θ scan of (0002) diffraction plane of AlGaN/GaN heterostructures on 200 mm Si(111). The inset shows the rocking curves of (002) and (102) planes giving a measure of tilt and twist in such large area epiwafer.

FIG. 3. (a) Variable temperature micro-PL spectra from AlGaN/GaN heterostructure on Si(111) recorded under 266 nm laser line excitation. The broader PL at higher energy side appears from the top thin AlGaN barrier. (b) PL spectra excited under 325 nm laser line show a much uniform GaN luminescence profile across the 200 mm wafers.

FIG. 4. (a) Room temperature micro-Raman spectra from AlGaN/GaN heterostructure on Si(111) recorded under 325 nm laser line excitation from various positions across the wafers. (b) Variable temperature Raman spectra excited under 325 nm showing the presence of disorder activated (DA), interfaces modes IF1 and IF2, and AlGaN A_1(LO) modes. The inset shows peak

fitting showing the position of AlGaN A1(LO) at 776.2cm^{-1}. The quasi-LO (Q-LO) phonon of GaN appears at low temperature.

Figure 1

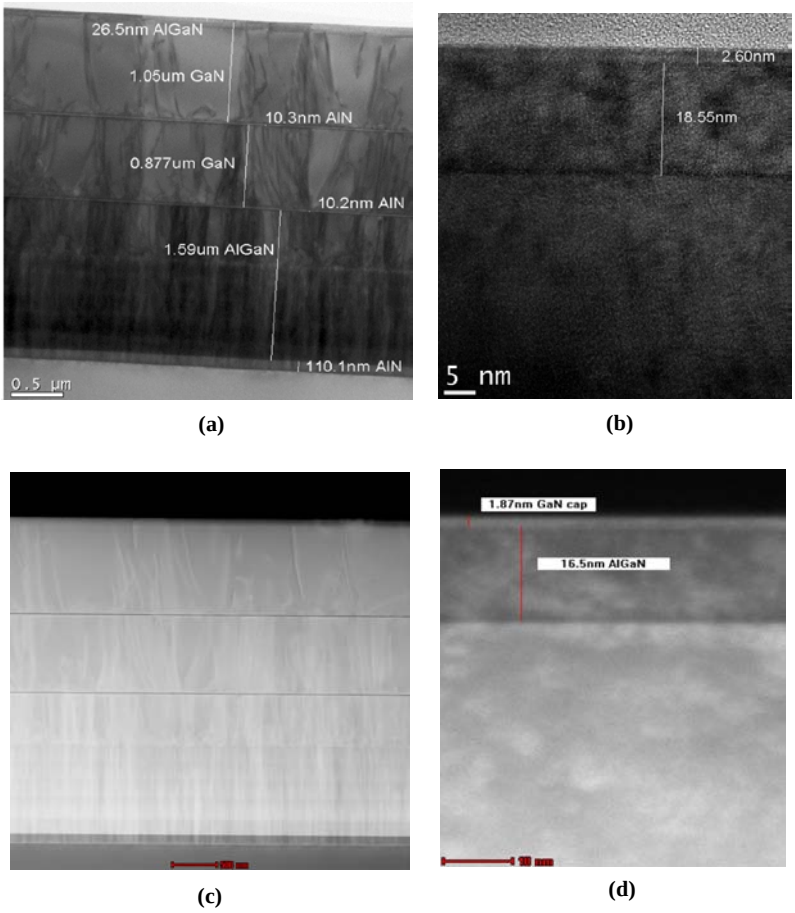

(a) **(b)**

(c) **(d)**

Figure 2

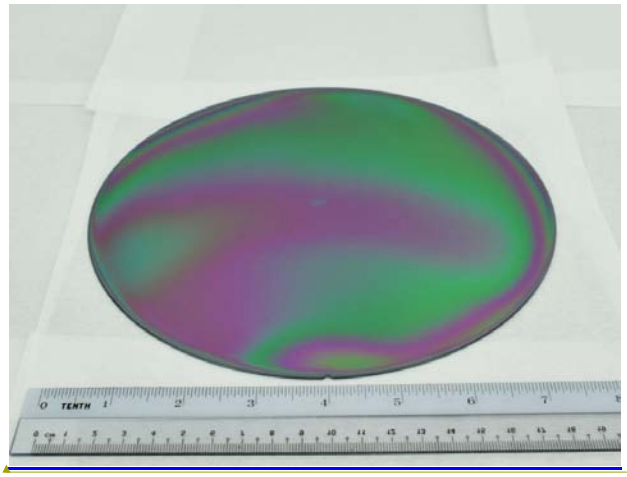

(a)

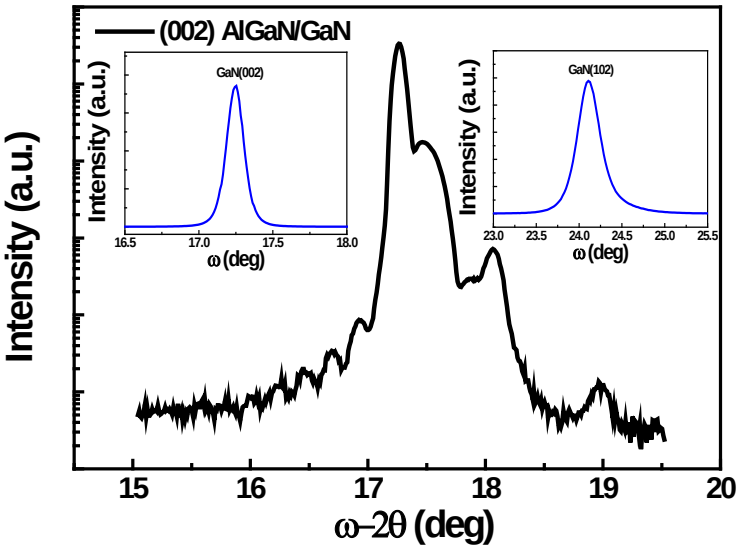

(b)

Formatted: Font: Bold

Formatted: Centered

Formatted: Font: Not Bold

Figure 3

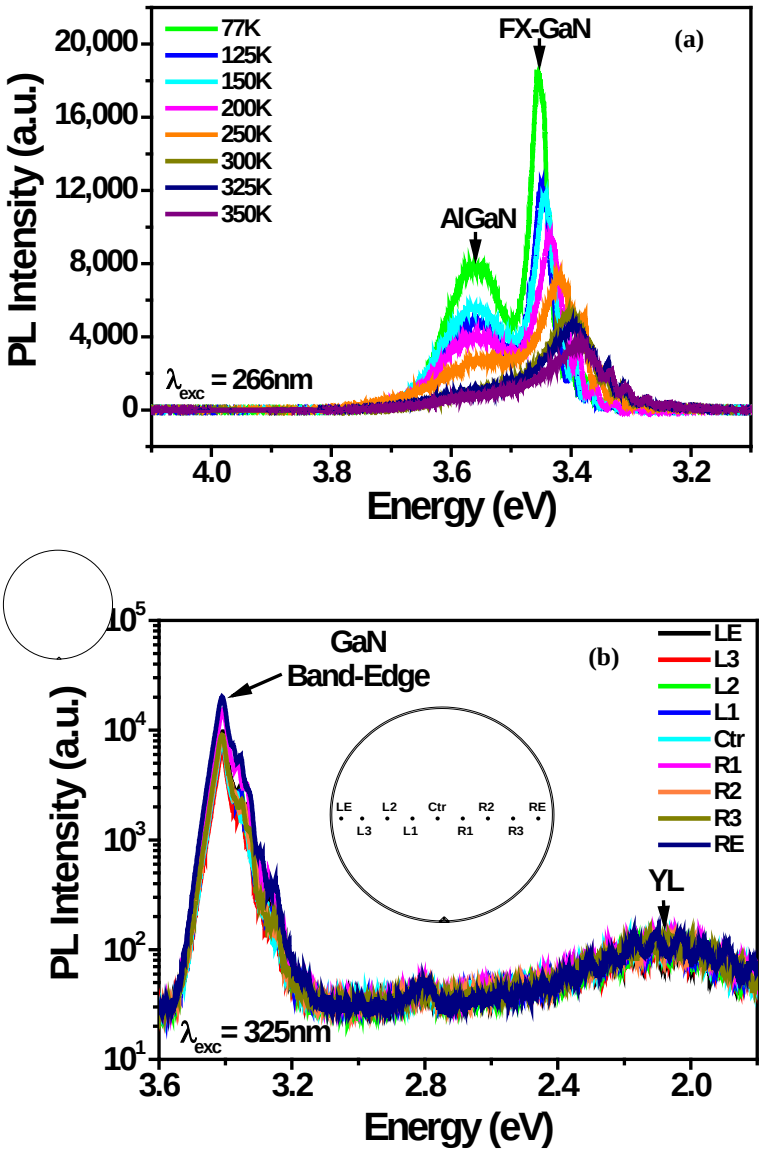
77K
125K
150K
200K
250K
300K
325K
350K
FX-GaN
AlGaN
(a)
PL Intensity (a.u.)
20,000
16,000
12,000
8,000
4,000
0
λexc = 266nm
4.0
3.8
3.6
3.4
3.2
Energy (eV)
GaN
Band-Edge
(b)
LE
L3
L2
L1
Ctr
R1
R2
R3
RE
YL
PL Intensity (a.u.)
10^5
10^4
10^3
10^2
10^1
λexc = 325nm
3.6
3.2
2.8
2.4
2.0
Energy (eV)

Figure 4

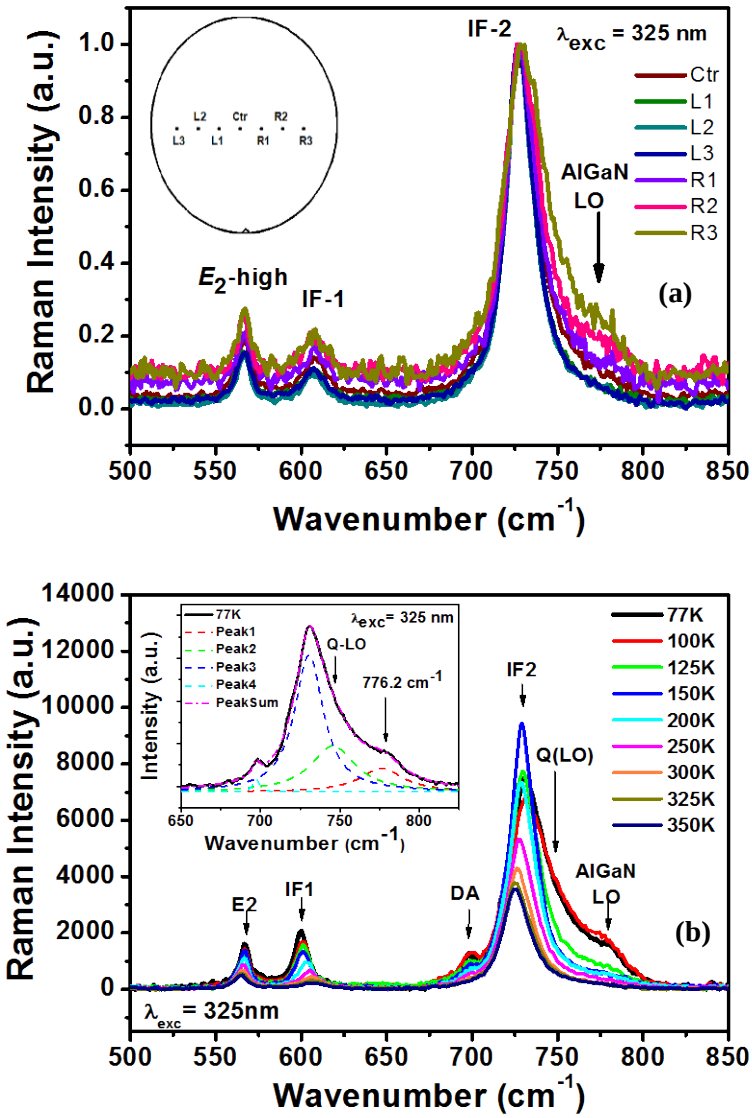
Raman Intensity (a.u.)
Wavenumber (cm-1)
IF-2
λexc = 325 nm
Ctr
L1
L2
L3
R1
R2
R3
AlGaN
LO
E2-high
IF-1
(a)
77K
Peak1
Peak2
Peak3
Peak4
PeakSum
λexc= 325 nm
Q-LO
776.2 cm-1
Intensity (a.u.)
IF2
Q(LO)
100K
125K
150K
200K
250K
300K
325K
350K
E2
IF1
DA
(b)
λexc = 325nm